ACS NANO

www.acsnano.org

ARTICLE

Waveguide and Plasmonic Absorption-Induced Transparency

Xiaolan Zhong,[†] Sergio G. Rodrigo,[‡,§] Lei Zhang,[†] Paolo Samorì,[†] Cyriaque Genet,[†] Luis Martín-Moreno,[§] James A. Hutchison,[*,†] and Thomas W. Ebbesen[†]

[†]ISIS & icFRC, Université de Strasbourg and CNRS, 8 allée Gaspard Monge, 67000 Strasbourg, France

[‡]Centro Universitario de la Defensa, Carretera de Huesca s/n, E-50090 Zaragoza, Spain

[§]Instituto de Ciencia de Materiales de Aragón and Departamento de Física de la Materia Condensada, CSIC-Universidad de Zaragoza, E-50009 Zaragoza, Spain

Supporting Information

ABSTRACT: **Absorption-induced transparency (AIT) is one of the family of induced transparencies that has emerged in recent decades in the fields of plasmonics and metamaterials. It is a seemingly paradoxical phenomenon in which transmission through nanoholes in gold and silver is dramatically enhanced at wavelengths where a physisorbed dye layer absorbs strongly. The origin of AIT remains controversial, with both experimental and theoretical work pointing to either surface (plasmonic) or in-hole (waveguide) mechanisms. Here, we resolve this controversy by carefully filling nanoholes in a silver film with dielectric material before depositing dye on the surface. Our experiments and modeling show that not only do plasmonic and waveguide contributions to AIT both exist, but they are spectrally identical, operating in concert when the dye is both in the holes and on the surface.**

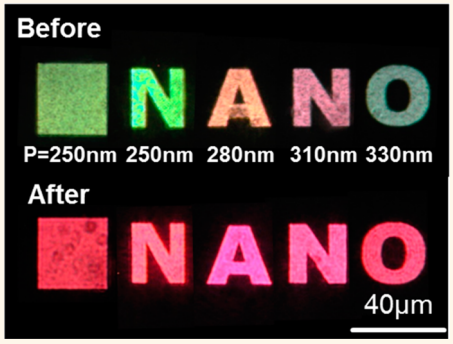

KEYWORDS: *surface plasmons, absorption-induced transparency, nanoscale apertures, plasmonic hole arrays, waveguides*

When nanoholes in a gold or silver film are covered by a dense layer of dye, a transparency is induced at wavelengths where the dye absorbs strongly.[1] This absorption-induced transparency (AIT) has a sharp onset at the dye absorption band maximum, leading to the surprising effect that a red light-absorbing dye appears, when viewed through the holes, red.

AIT is highly sensitive to the metal film used, being most intense on silver or gold, suggesting a possible role for surface plasmon polaritons (SPPs). The large scattering cross sections and interfacial field intensity of SPP resonances means they often dominate the light response of nanostructures, being implicated in enhanced absorption and emission,[2−10] refractive index shifts,[11−14] and Raman scattering,[15] of adsorbed molecules, in Fano resonances,[16,17] and in optical leakage through aperture arrays at wavelengths far above cutoff for waveguide propagation.[18−20]

At the same time, however, AIT is weakly dispersive and present even for disordered groups of holes,[1] indicating a role for the local properties of each aperture, for example, their waveguide properties and in-hole Fabry−Pérot (FP) resonances.[21,22] Electron microscopy analysis in the original work showed that the dye was distributed not only on the metal surface, but also significantly filled the holes, and contributions to AIT from both a change in the refractive index inside the holes, and from molecule-SPP interactions at the surface, were inferred.[1]

Later interpretations of AIT have been similarly divided. It has been speculated to be a hybrid analogue of electromagnetic induced transparency (EIT),[23] and plasmon induced transparency (PIT)[24] demonstrated in metamaterials.[25] The critical coupling effect[26] may play a role. However, AIT has been shown to occur in the complete absence of resonant SPPs via guided modes through the dye-filled holes[27] even for subwavelength holes in a perfect electrical conductor.[28] A plasmonic guided mode within the dye layer along the surface has also been proposed to account for the effect.[29]

Here, we seek to resolve this controversy by precisely filling subwavelength diameter nanoholes in a silver film with dielectric material such that surface and in-hole contributions to AIT can be isolated. We show that AIT has in fact both plasmonic and in-hole waveguide contributions. The origin in each case is a strong perturbation of the dispersion relation of the relevant propagation constant by the molecular absorber, but with an apparent contradiction of its own. Although filling the hole with dye *reduces* the evanescence of the waveguide mode to favor propagative transmission in the AIT spectral

Received: January 28, 2016
Accepted: April 11, 2016

DOI: 10.1021/acsnano.6b00709
ACS Nano XXXX, XXX, XXX−XXX

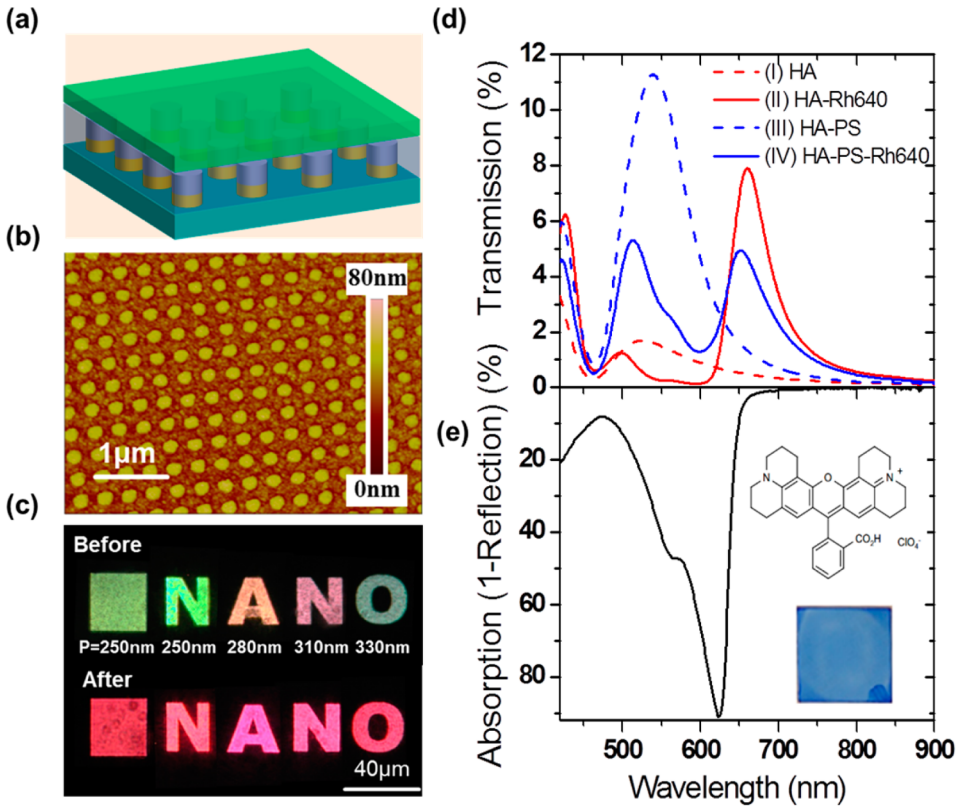

Figure 1. (a) Schematic subwavelength square hole array milled in a silver film (indicated in gray) on a glass substrate (blue) filled with 80 nm LiF (yellow) and then 120 nm polystyrene (mauve), upon which is deposited 40 nm of Rhodamine 640 (green). (b) AFM image of the dielectric-filled silver hole array. The polystyrene slightly overfills the holes by ~10 nm. (c) Optical micrograph of subwavelength silver hole arrays of various periods (P) in the absence (before) and presence (after) of a Rhodamine 640 film deposited on top. (d) Transmission spectra of a square hole array (period 250 nm, hole diameter 100 nm) milled in a 200 nm thick Ag film in the absence (dash curves) and the presence (solid curves) of Rhodamine 640 when the holes are filled with 80 nm LiF and then 120 nm polystyrene (blue curves) or unfilled (red curves) before depositing the dye. (e) Absorption spectrum (measured as 1-reflection) of a 40 nm film of Rhodamine 640 on an unstructured 200 nm thick silver film. Inset: the structure of Rhodamine 640 and a photograph showing the blue color of a 40 nm Rhodamine 640 film on a glass substrate viewed in transmission.

region, placing the dye film on the surface *increases* the evanescence of the SPP mode perpendicular to the interface (i.e., making it more surface bound) in the same spectral region. The latter nevertheless also favors transmission by leakage of the SPP through the subwavelength holes. Thus, the two contributions to the induced transparency are finally spectrally identical and reinforce one another.

RESULTS AND DISCUSSION

We developed a technique for the precise filling of 100−160 nm diameter holes in 200 nm silver films with dielectric (80 nm of LiF and 120 nm of polystyrene, PS), such that a neat 40 ± 5 nm film of the dye Rhodamine 640 could be physisorbed exclusively on the top surface of the holes (see schematic in Figure 1a and Methods). Further fabrication details and SEM structural analysis, together with details of optical measurements and simulation methods, are included in the Supporting Information (SI, Section S1). Atomic force microscopy (AFM) characterization confirmed that the LiF and PS fully filled the holes with the upper PS layer even slightly protruding out of the holes by ~10 nm (Figure 1b). Importantly, the dielectric-filled holes have an effective refractive index $n \sim 1.5$ (weighted average of $n_{LiF} = 1.39$ and $n_{Polystyrene} = 1.59$) in the visible region, similar to the background index when the holes are filled with dye material (as estimated by simulations, see Methods and SI, Section S2). Our structure therefore provides a close model to the canonical AIT system except the dye absorption resonance is absent inside the hole.

We fabricated ordered arrays of dielectric-filled nanoholes which can launch grating SPPs, and also disordered groups of dielectric-filled holes for which SPPs are only locally associated with the holes. We study their optical properties sequentially next.

Periodic Holes Array. The transmission spectrum of a square hole array of 100 nm diameter holes (unfilled) milled by focused ion beam (FIB) in a 200 nm thick Ag film with a period of 250 nm (red dashed curve) is shown in Figure 1d. SPP modes on subwavelength metallic hole arrays are generated via Bragg scattering according to[30]

$$|\vec{k}_{SPP}| = |\vec{k}_{||} + i\vec{G}_x + j\vec{G}_y| \quad (1)$$

where $\vec{k}_{||}$ is the in-plane wave vector component of the incident light, $\vec{k}_{SPP}$ is the SPP wave vector, and $\vec{G}_x$ and $\vec{G}_y$ are the reciprocal lattice vectors $|\vec{G}_x| = |\vec{G}_x| = 2\pi/P$, where P is the lattice period), and i and j are integers. Grating coupling ensures momentum matching between incident light and the surface mode according to the condition

DOI: 10.1021/acsnano.6b00709
ACS Nano XXXX, XXX, XXX−XXX

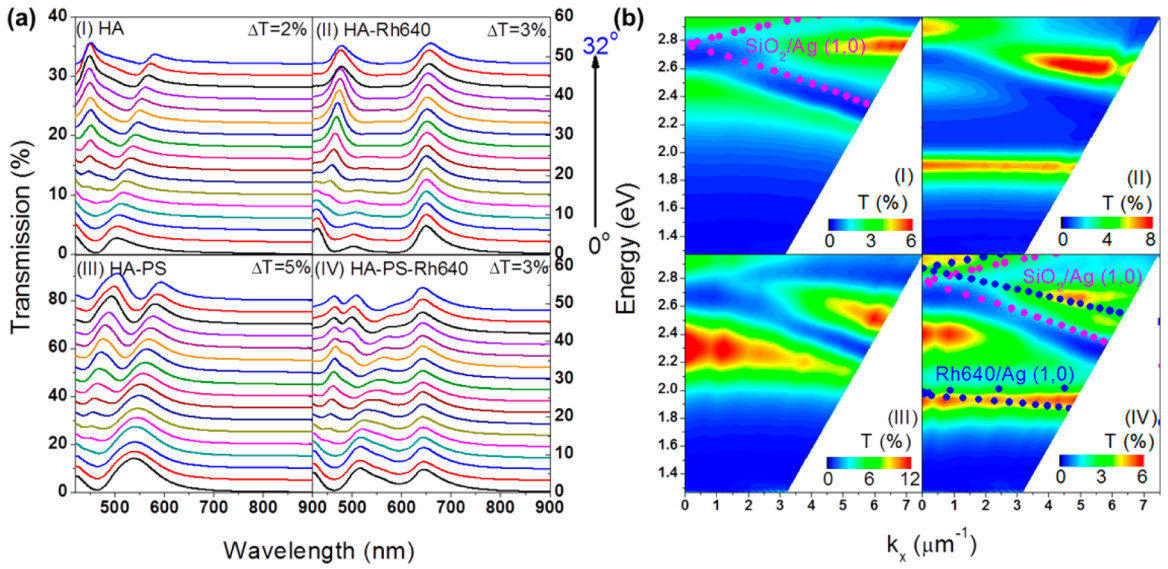

Figure 2. (a) Transmission spectra of a square hole array (period 250 nm, hole diameter 100 nm, Ag film thickness 200 nm) with a Rhodamine 640 film recorded as a function of the angle of *p*-polarized incident radiation (0° ~ 32° with spectra offset by ΔT) and (b) the corresponding dispersion plots where ($k_x = k_{\|} = nk_0 \sin\theta$). The data for the bare array with unfilled (I) and dielectric-filled (III) holes are juxtaposed with that of the same arrays with Rhodamine 640 both in the holes and on the surface (II), and just on the surface (IV). The solid circles are the theoretical fit for the (1,0) SPP between SiO_2 and silver (purple) and between Rhodamine 640 and silver (blue) calculated from eq 1 and 2.

$$\vec{k}_{SPP} = \vec{k}_0 \sqrt{\frac{\varepsilon_d \varepsilon_m}{\varepsilon_d + \varepsilon_m}} \quad (2)$$

where $\vec{k}_0$ is the wave vector of the incident light in free space, and ε_d and ε_m are the permittivities of the (infinite) dielectric and the metal media, respectively. Only the transmission peak associated with the (1,0) SPP resonance on the glass/metal interface of the hole array is visible at 520 nm for the 250 nm array. The transmission spectrum of a dielectric-filled hole array (blue dashed curve) is also shown in Figure 1d. Its transmission is ~10 times higher, whereas its (1,0) SPP resonance energy is red-shifted by 20 nm. The enhanced transmission is due to the increased refractive index in the holes effectively widening the hole for incident radiation (the emergence of Fabry–Pérot resonances near 550 nm in the dielectric-filled holes are discussed further below).

When a Rhodamine 640 film is directly spin-cast on a hole array without dielectric filling, the dye is distributed inside the holes and on the surface simultaneously. AIT is clearly visible as a new and intense transmission with a sharp onset at 612 nm (Figure 1d, red solid curve) and peaking at 659 nm, while on the blue side of the Rhodamine absorption, transmission is suppressed. When the same Rhodamine film is spun onto an array of dielectric-filled holes, one observes weaker yet qualitatively similar spectral changes. Again the transmission (blue solid curve) is enhanced with an onset at 612 nm and a peak at 652 nm, and suppressed on the blue side of the absorption. The salient feature of AIT, transmission enhancement on the red side of the dye absorption maximum and damping on the blue side, is clear in both cases considering the 620 nm absorption peak of the Rhodamine 640 layer on flat silver (Figure 1e, the dye absorption peak is red-shifted by 10 nm compared to that on glass). AIT is not simply a filtering of the array transmission by the dye, as will also be shown by numerical simulations later, and we checked that the spectra did not exhibit any contribution from fluorescence. An optical micrograph of the transmission of subwavelength hole arrays of various periods in silver without (top) and with (bottom) a Rhodamine 640 film on top is shown in Figure 1c. The pink-red color of the AIT transmission dominates the colors of the original plasmonic resonances, and compares with the blue colored transmission of the same dye film on glass (inset, Figure 1e).

Another characteristic feature of AIT is its weakly dispersive nature. This is illustrated in Figure 2, showing transmission spectra as a function of the angle of *p*-polarized incident radiation for the four arrays discussed in Figure 1d (see Figure 2a). The corresponding ω/k dispersion relations are shown in Figure 2b. In the absence of Rhodamine 640, for unfilled (I) or dielectric-filled (III) holes, the SPP peaks shift as the probe angle is increased, corresponding to an increased in-plane momentum of the incident field and in accordance with eq 1 ($k_x = k_{\|} = nk_0 \sin\theta$). When Rhodamine 640 is deposited on the arrays, either on the surface and in the holes (II), or only on the surface (IV), the resulting AIT peak at ~650 nm is in both cases observed to disperse very weakly compared to the SPP modes. The slight blue shift of ca. 8 nm in the AIT peak when the molecules are dispersed only on the surface of the array is also constant with angle. The same weakly dispersive behavior of the AIT mode is observed when the period of the arrays is varied, though some broadening is observed at higher periods (see SI, Section S3).

To better understand the surface contribution to AIT, numerical simulations were undertaken using the finite difference time domain (FDTD) method as outlined in ref 27. A Drude–Lorentz model was employed to simulate the permittivity of the silver film, giving a good fit to the experimental response in the visible range.[31] For the Rhodamine 640 dye layer we modeled the dielectric response $\varepsilon_d(\omega)$ using a two-component Lorentz model

DOI: 10.1021/acsnano.6b00709
ACS Nano XXXX, XXX, XXX–XXX

$$\varepsilon_d(\omega) = \varepsilon_{host} - \sum_{j=1}^{2} \frac{\Delta\varepsilon_j \Omega_j^2}{\omega^2 - \Omega_j^2 + i\Gamma_j\omega} \quad (3)$$

where Ω_j is the absorption maximum, $\Delta\varepsilon_j$ is the peak oscillator strength, and Γ_j the line width of component j, and ε_{host} is the host (background) dielectric constant. We then used an analytical expression for calculating the absorption in an unperforated silver film coated with a 40 nm Rhodamine 640 layer to define a set of material parameters which fairly reproduce the main absorption features observed in Figure 1d. We obtained: ε_{host} = 2.25, $\Delta\varepsilon_1$ = 0.184, Ω_1 = 2.023 eV, Γ_1 = 0.092 eV, $\Delta\varepsilon_2$ = 0.095, Ω_2 = 2.217 eV, and Γ_2 = 0.230 eV. The simulated real and imaginary parts of the permittivity of the dye layer are shown in Figure 3a.

Simulated spectra for a bare 330 nm period hole array (black curve) and for the same array when the holes are filled with dielectric (green curve) are shown in Figure 3b (for further computational details see SI, Section 1, and ref 32 and references therein). The experimentally observed red shift and increased intensity in the (1,0) SPP resonance when the holes are filled with dielectric are well reproduced. The additional shoulder on the peak near 500 nm is due to coupling between the glass-Ag SPP and a Fabry–Pérot mode in the dielectric-filled holes. The spectrum of the FP mode is calculated for a single d = 120 nm dielectric-filled hole in the SI, Section S4. It appears close to the cutoff wavelength (ca. 548 nm) as estimated from the propagation constant for holes in silver both by FDTD methods and the implicit analytical expression for circular waveguides.[33]

The red curve in Figure 3b is the simulated spectrum obtained by multiplying the dielectric-filled hole array transmission spectrum by the transmission of a 40 nm Rhodamine 640 film in air (without substrate). In other words, it is the spectrum obtained if the surface dye layer acts only to filter the array transmission. Clearly the features of AIT are not reproduced by this "trivial" model.

The simulated spectrum obtained for the 330 nm period dielectric-filled hole array with Rhodamine 640 layer on top is shown in Figure 3c (red curve) where it is compared to the experimental result (blue curve). The AIT peak at 653 nm is clearly reproduced in the simulations, even though its intensity relative to the grating (1,0) SPP at 595 nm is reduced compared to experiments. The latter SPP mode is strongly damped in simulations of 350 and 390 nm period arrays. In general a much higher AIT intensity is observed experimentally than in the simulations for a range of other period arrays (SI Section S3, Figure S4). These differences between experiment and simulation for the same nominal parameters may be due to irregularities in the hole shape, size and filling, or the dye layer thickness in the fabricated structures. Variation in refractive indices of the materials going from bulk to finite volumes can also play a role (for example, a closer match to the observed ratio of the (1,0) SPP and AIT peaks is obtained if calculations are done for a hole filled only with PS, n = 1.59, see SI, Section S2). In agreement with previous studies that showed a linear relationship between dye film absorbance and AIT transmission intensity,[1] the calculated AIT intensity reduces in favor of the SPP mode as the concentration of the Rhodamine 640 on the surface is reduced (see SI, Section S5).

Simulations in Figure 3d emphasize two further points. First, when the dye is dispersed both in the holes and on the surface of the same hole array structure (green curve) the AIT signal is much stronger than when the dye is dispersed only in the holes (red curve) indicating that contributions to AIT occur both on the surface and in the hole and are additive. Second, when dye is only present on the surface but with air inside the holes (black curve, Figure 3d) the AIT peak is extremely weak, as reported previously.[27] Thus, having a background dielectric constant of ~1.5 inside the holes is crucial in order to observe a strong surface contribution to AIT.

Importantly, calculated near-field maps of the electric field at the AIT peak (653 nm) for the same period 330 nm dielectric-filled hole array with dye on top clearly show a SPP-like propagation pattern (Figure 4a–c). The E-field component perpendicular to the surface displays the typical fringes of the

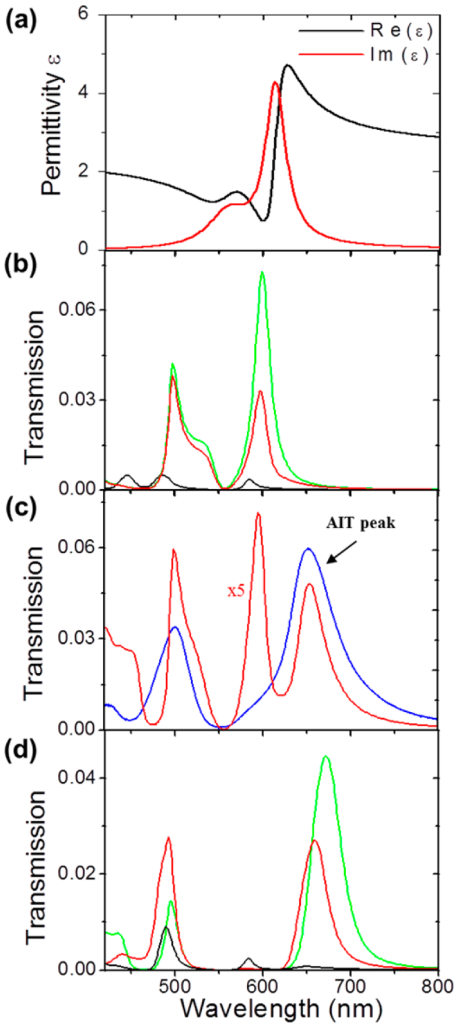

Figure 3. (a) The calculated permittivity of the 40 nm Rhodamine 640 layer on silver. (b) Calculated transmission spectra of a square hole array (period 330 nm, hole diameter 120 nm) in a 200 nm thick Ag film when the holes are unfilled (black curve) and filled with 80 nm LiF and then 120 nm polystyrene (green curve). The red curve is the transmission expected if a 40 nm Rhodamine 640 film acted only as a filter for the dielectric-filled hole array. (c) Calculated transmission for the same dielectric-filled hole array with a 40 nm Rhodamine 640 dye layer on the surface (red curve), the experimental result for a similar array (period 330 nm, hole diameter 100 nm) is included (blue curve). (d) Calculated transmission spectra for the same hole array in which the dye is present both on the surface and in the holes (green curve), only in the holes (red curve), and only on the surface with air in the holes (black curve).

DOI: 10.1021/acsnano.6b00709
ACS Nano XXXX, XXX, XXX–XXX

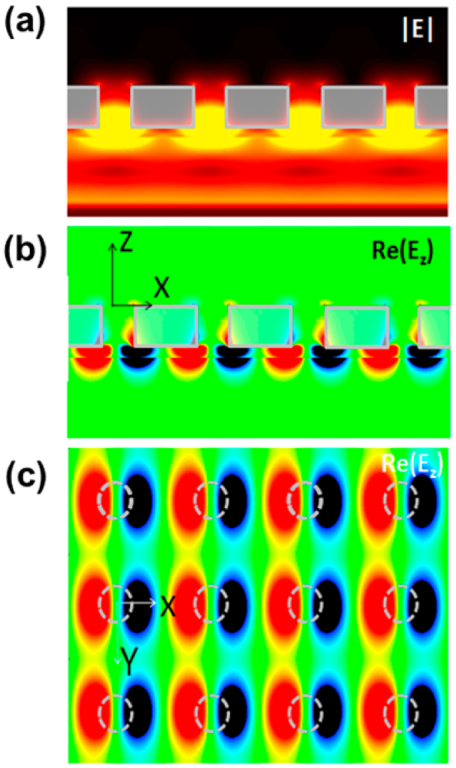

Figure 4. (a)−(c) Calculated near field maps of the electric field (E) at the AIT maximum ($\lambda \sim 653$ nm) for several unit cells along the x direction on the x−z plane. Field amplitude and Re(E_z) are represented in (a) and (b), respectively (Re(E_z) > 0 red, Re(E_z) < 0 blue Re(E_z) = 0 green). Panel c shows Re(E_z) on the XY plane located a few nanometers below the Rhodamine 640 film. The incident field is polarized along the x axis, incident from the Rhodamine 640 side (bottom hole array surface). The circles indicate the spatial location of holes as a guide to the eye.

(1,0) SPP for that configuration (panels a and b), and strong confinement normal to the surface as expected for a surface mode (the dye layer is on the bottom side in panels a and b). The different interfaces are clearly distinguished due to the refractive index change from air to Rhodamine 640, from Rhodamine 640 to PS inside the hole, and even inside the hole going from PS to LiF.

Disordered Groups of Holes. The effect of periodicity and its associated grating SPP modes can be removed by studying disordered groups of holes, also allowing one to clearly assess the effect of hole diameter on AIT. The spectra of the disordered groups of unfilled holes milled by FIB in a 200 nm thick Ag film (4.2 holes/μm^2, see SEM images in SI, Figure S2) are broad and relatively featureless due to SPP modes associated with the individual holes, through a process where each hole contributes to transmission by scattering of SPPs generated from neighboring holes (dashed curves in Figure 5a).[34]

As was observed for the periodic arrays (Figure 1b) filling the holes with dielectric increases the transmission intensity (here 4−5 times, dashed lines Figure 5b). The dielectric-filled holes also show more pronounced, red-shifted, resonances attributed to Fabry−Pérot modes near the cutoff wavelength (SI, Section S4) and this broad envelope continues to shift to the red as the hole diameter increases (Figure 5b). When the Rhodamine 640 layer is deposited such that the dye is both in the holes and on the surface (Figure 5a, solid lines), or only on the surface (Figure 5b, solid lines), characteristic and qualitatively similar AIT features are once again apparent in each case. Transmission enhancement occurs from the maximum of the dye absorption while to the blue of the resonance transmission is suppressed, recovering again below ∼500 nm. The effects are again greatest when the molecules are both on the surface and in the hole. AIT shows a strong dependence on hole diameter in both cases, with the full width at half-maximum of the AIT peak broadening substantially with increasing hole diameter. The same broadening of AIT with hole diameter is apparent for periodic arrays (see SI Section S3, Figure S4, and Section S6).

An isolated hole was used to simulate the spectra of the disordered groups of holes. When the dye is present in the hole and on the surface, the simulation reproduces the AIT peak and its hole diameter dependence (Figure 5c). As was shown previously, calculations predict that whenever dye is in a single, isolated hole, AIT is observed due to in-hole waveguiding (see also SI, Section S4). However, for single a dielectric-filled hole with dye only on the surface, the experimentally observed AIT is not reproduced by the calculations (Figure 5d). As already mentioned, near-neighbor holes facilitate efficient transmission through disordered groups of holes as they rescatter SPPs launched locally at a single hole.[34] Such possibilities are of course absent in simulations of an isolated hole, thus the failure to reproduce the surface AIT in such calculations suggests again a plasmonic contribution (i.e., SPPs launched locally at the AIT energy are re-emitted by near-neighbor holes). The inability of a single, isolated hole to simultaneously act as a source and rescatterer of SPPs can be concluded from calculations of an isolated hole in silver compared to that in a perfect electric conductor (PEC, see SI, Section S4 for details). Experiments on disordered groups of dielectric-filled holes with densities in the range 1.6−4.2 holes/μm^2 did not show any clear trend regarding hole number-normalized AIT intensity and hole density. Further experiments at much lower hole densities are required to confirm the predicted behavior of a single isolated hole with respect to AIT.

Calculation of the Relevant Propagation Constants. The existence of SPPs at the AIT energy can be inferred by calculating the propagation constant for the SPP (k_{SPP}) at an unstructured interface between infinite metal and dye media. This was done using eq 2 as an approximation for the 40 nm thick dye layer on silver, inserting the estimated permittivities discussed earlier. k_{SPP} is shown in Figure 6a (blue curve) together with the light cone shaded in gray ($n_{Background}$ = 1.5, black curve). k_{SPP} follows the light line in the near-IR as the metal approximates a perfect conductor and the SPP is light-like and weakly bound to the interface. As the dye absorption resonance is approached, however, k_{SPP} deviates away from the light line deep into the evanescent region (compared with k_{SPP} calculated for an infinite n = 1.5 dielectric/silver interface, green curve Figure 6a). The mode is strongly surface-bound with a large imaginary part of k_Z for a strong SPP decay normal to the interface. The SPP is weakly dispersive particularly near 627 nm where k_{SPP} undergoes anomalous dispersion, intersecting the light cone at 606 nm, very close to the observed onset of AIT. Conversely, in the region between 606 and 478 nm, k_{SPP} lies within the light cone and a surface-bound mode is not defined (eq 2). The propagation length for the SPP, L_{SPP}, the inverse of the imaginary part of k_{SPP}, increases rapidly on the red side of the dye absorption with a sharp onset near the dye absorption maximum (Figure 6a, red curve).

DOI: 10.1021/acsnano.6b00709
ACS Nano XXXX, XXX, XXX−XXX

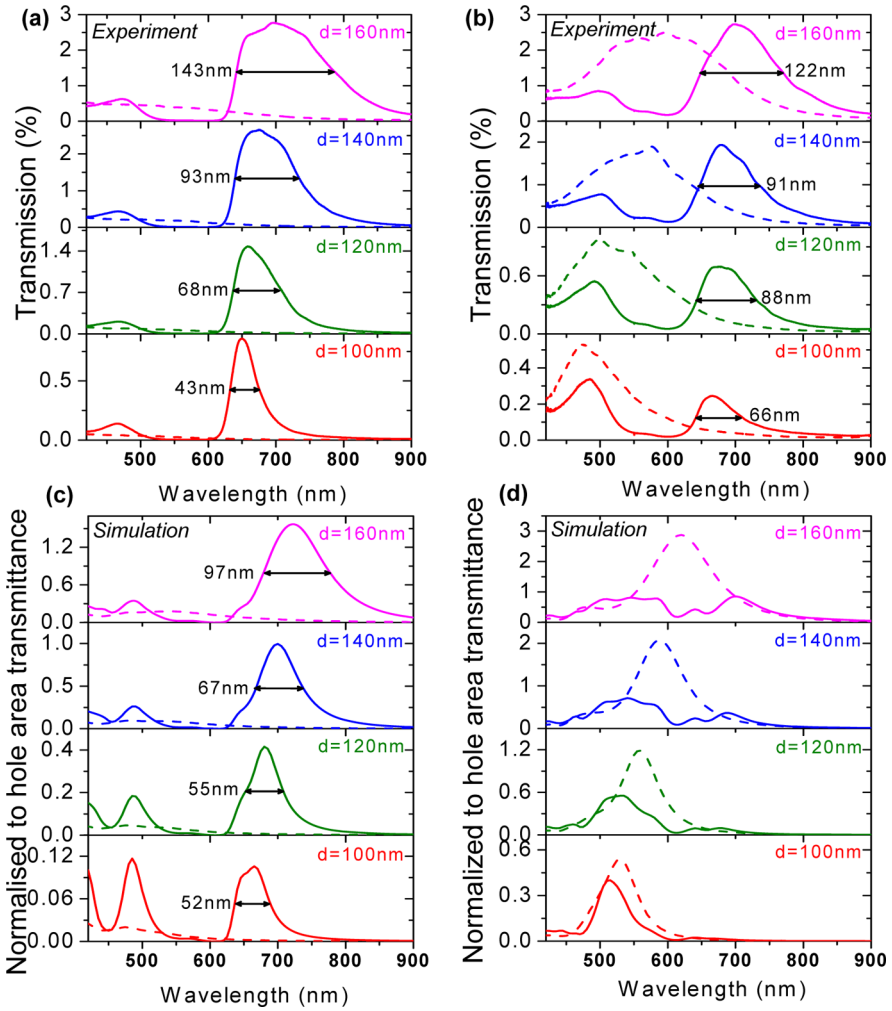

Figure 5. Transmission spectra of disordered groups of holes (hole density: 4.2 holes per μm^2) milled in a 200 nm thick Ag film recorded in the absence (dash lines) and presence (solid lines) of a 40 nm layer of Rhodamine 640. The disordered groups of holes were (a) initially unfilled or (b) dielectric-filled and the hole diameter varied as indicated. The full width at half-maximum of the AIT peak is also indicated. (c) and (d) Calculated transmission spectra for an isolated hole with parameters corresponding to (a) and (b), respectively.

There is excellent correspondence between the experimentally observed surface contribution to AIT and the spectral regions in which a surface plasmon is well defined according to eq 2, confirming the evidence for a surface mode already provided by the FDTD simulations. Transmission through metallic holes beyond cutoff occurs by leakage of the SPP fields at the interface, whether it involves local or grating SPPs, is most efficient at energies where the SPP is strongly bound to the interface, that is, where k_{SPP} lies deep in the evanescent region. The anomalous dispersion of k_{SPP} between 627 and 608 nm means that for a periodic array, a large range of incident angles and array periods satisfy the grating coupling condition (eq 1) for a SPP with wavelength just to the red of the dye absorption maximum. This is also the region where L_{SPP} is rapidly increasing. Taken together these points account for the weakly dispersive and increasingly intense SPP mode with onset at the absorption maximum of the dye. k_{SPP} calculated from eq 2 is superimposed on the dispersion of the period 250 nm dielectric-filled hole array with dye on top in Figure 2b(IV). The agreement with the observed AIT peak is excellent though splitting of k_{SPP} at higher probe angles/periods is observed only as a broadening of the AIT peak in experiments (see Figure 2 and SI, Section S3).

For disordered group of holes, the launching of SPPs locally at each hole at the AIT energy, followed by re-emission through neighboring holes is reasonable given the increasing SPP propagation length at the AIT peak (Figure 6a) relative to the hole separation (4.2 holes/μm^2). We recall here that the AIT line-shape broadened with increasing hole diameter when the Rhodamine 640 was only present on the surface of the disordered holes (Figure 5b). This is because the probability of tunneling of SPP modes at the hole/dye interface has a Fabry–Pérot functional form (see eq 2 in ref 20) determined on the propagation constant for a dye-filled waveguide.

For completeness, we calculate this propagation constant, following Rodrigo et al., to simulate the in-hole guided mode contribution to AIT for a d = 100 nm diameter hole filled with Rhodamine 640 (Figure 6b).[27] The permittivity of the dye (ε_d) is inserted into the expression for the propagation constant (k_Z) of a circular waveguide in a perfect metal (perfect electrical conductor)

$$k_z = \sqrt{\varepsilon_d k_0^2 - \omega_s^2} \tag{4}$$

where k_0 is the wave vector of the incident light in free space, $\omega_s^2 = (2\pi/k_x)^2 + (2\pi/k_y)^2$, k_x and k_y are the wave vector components along the x and y axes, respectively. If we consider

DOI: 10.1021/acsnano.6b00709
ACS Nano XXXX, XXX, XXX–XXX

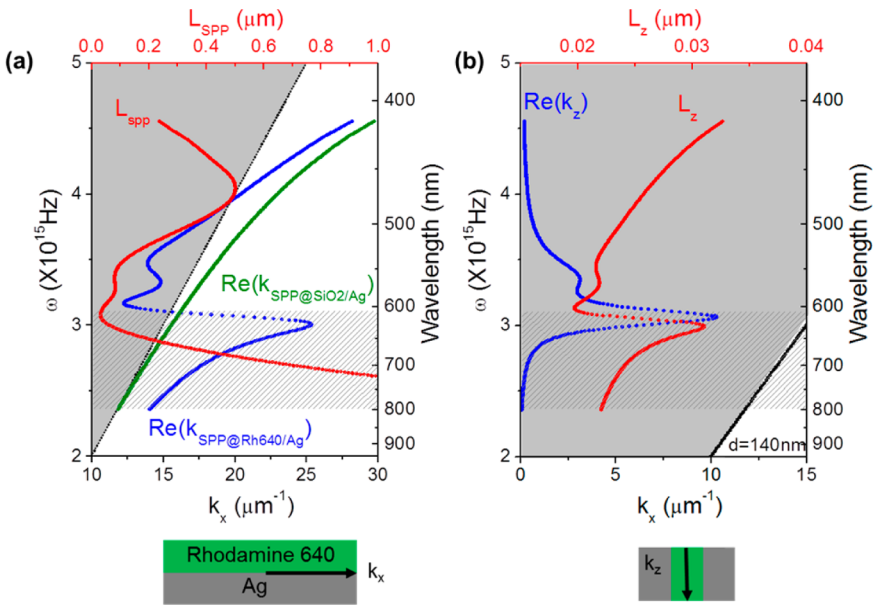

Figure 6. (a) **Propagation constant of the surface plasmon mode Re(k_{SPP}) at an interface between infinite silver and Rhodamine 640 media (blue curve, calculated from eq 2) and the propagation length of the SPP along the interface L_{SPP} = Im(k_{SPP})$^{-1}$/2 (red curve). k_{SPP} at a silver/silica interface is also included (green curve). The black curve corresponds to the light cone in the dye medium ($n_{Background}$ = 1.5). (b) Real part (blue curve) of the in-hole waveguide propagation constant from eq 4 and the propagation length along the waveguide L_z = Im(k_z)$^{-1}$/2, and the light cone in the dye medium (black curve, $n_{Background}$ = 1.5). The hatched area in (a) and (b) corresponds to the AIT region.**

the first mode of the transverse electric (TE) field solution, eq 4 can be written as $k_z = \sqrt{\varepsilon_d k_0^2 - (1.84/r)^2}$, where r is the radius of waveguide. The high value of Re(k_Z) (blue curve, Figure 6b) reduces evanescence inside the holes, favoring propagative transmission and this is also the region where L_z is rapidly increasing, corresponding well with the observed AIT spectral region. The same analysis for larger hole diameters predicts the observed AIT line-shape broadening, further confirming the predictions of Rodrigo et al.[27]

To further clarify, the AIT phenomenon occurs at wavelengths where the real part of the propagation constant presents strong frequency dispersion, due to a change in the dielectric constant produced by the molecules. The appearance of AIT at the red side of the molecular absorption wavelength instead of on the blue side is due to the asymmetric behavior of the propagation constant around the Rhodamine absorption energy. Within the normal dispersion region (red wavelength side) light transmission is possible given the moderate values of the propagation length, whereas absorption dominates the anomalous dispersion region (blue wavelength side). Outside the normal and anomalous spectral windows the influence of the dye layer weakens and far from the resonance the thin layer behaves like a lossless dielectric.

CONCLUSIONS

In summary, our experiments and modeling show that AIT can have contributions from both surface (plasmonic) and in-hole guided modes, as predicted individually by Yeh et al.[29] and Rodrigo et al.,[27] respectively. The region slightly to the red of the dye absorption, where the imaginary part of the propagation constant drops sharply but the real part remains reasonably large, is critical. Considering a dye-filled hole as a circular waveguide, k_z becomes *less* evanescent in this region favoring propagation through the hole. When the dye is on the surface, k_{SPP} bends away from the light line in this region, becoming more surface bound (k_Z *more* evanescent for the surface mode), which is the criteria for efficient transmission by SPPs through subwavelength holes.[27] Thus, though their origins are different, both in-hole and surface AIT occur at the same spectral region and reinforce each other when a dye is dispersed both in the holes and on the surface. AIT offers flexibility for tuning either surface or waveguide mode energies on plasmonic nanostructured arrays simply by choice of a dye with strong absorption at a desired frequency. Given that the organic dye layer can easily be manipulated by optical and electrochemical means, AIT has further great potential for active control.

METHOD

Briefly, a 200 nm thick silver film was evaporated on glass, and holes 100−160 nm in diameter were milled by focused ion beam (FIB). An 80 nm thick LiF film was then deposited onto the sample by vacuum evaporation (root-mean-square surface roughness 3.25 nm) and a 350 nm thick polystyrene (PS) film spin-coated on top from toluene. The PS film was then carefully etched by oxygen plasma until the holes were just filled (∼120 nm PS), with the metal surface still protected by LiF. The LiF layer on the metal surface could then easily be washed away using distilled water to give a dielectric-filled hole array. Finally, a 40 ± 5 nm Rhodamine 640 layer was spin-cast on the surface from a concentrated methanol solution which cannot dissolve PS (Rhodamine 640 was obtained from Exciton company, we estimate a Rhodamine 640 film density approaching ca. 1 molecule/nm^3 based on the density of the related Rhodamine 6G in crystalline form, see also SI, Section S1). The LiF/PS films were >95% transparent in the visible region, and we checked by simulation that the results herein are barely changed if the ratio of LiF to PS in the holes is varied (SI, Section S2). In other words, the presence of reflections inside the hole due to the different refractive indices of LiF and PS do not alter the conclusions.

DOI: 10.1021/acsnano.6b00709
ACS Nano XXXX, XXX, XXX−XXX

ASSOCIATED CONTENT

Supporting Information

The Supporting Information is available free of charge on the ACS Publications website at DOI: 10.1021/acsnano.6b00709.

Supporting Information includes further experimental methods, the effect of different dielectric fillings in the holes on AIT, the period dependence of AIT, single isolated hole AIT, the dye concentration dependence of AIT, and the hole diameter dependence of AIT. (PDF)

AUTHOR INFORMATION

Corresponding Author

*E-mail: hutchison@unistra.fr.

Notes

The authors declare no competing financial interest.

ACKNOWLEDGMENTS

We acknowledge support from the Spanish Ministry of Science and Innovation under project MAT2011-28581-C02, the ERC through the projects Plasmonics (GA-227557), Suprafunction (GA-257305), the International Center for Frontier Research in Chemistry (icFRC, Strasbourg), the ANR Equipex Union (ANR-10-EQPX-52-01), the Labex NIE projects (ANR-11-LABX-0058 NIE), and CSC (ANR-10-LABX- 0026 CSC) within the Investissement d'Avenir program ANR-10-IDEX-0002-02.

REFERENCES

(1) Hutchison, J. A.; O'Carroll, D. M.; Schwartz, T.; Genet, C.; Ebbesen, T. W. Absorption-Induced Transparency. *Angew. Chem., Int. Ed.* **2011**, *50*, 2085−2089.

(2) Lecarme, O.; Sun, Q.; Ueno, K.; Misawa, H. Robust and Versatile Light Absorption at Near-Infrared Wavelengths by Plasmonic Aluminum Nanorods. *ACS Photonics* **2014**, *1*, 538−546.

(3) Dintinger, J.; Klein, S.; Ebbesen, T. W. Molecule−Surface Plasmon Interactions in Hole Arrays: Enhanced Absorption, Refractive Index Changes, and All-Optical Switching. *Adv. Mater.* **2006**, *18*, 1267−1270.

(4) Geldmeier, J.; König, T.; Mahmoud, M. A.; El-Sayed, M. A.; Tsukruk, V. V. Tailoring the Plasmonic Modes of a Grating-Nanocube Assembly to Achieve Broadband Absorption in the Visible Spectrum. *Adv. Funct. Mater.* **2014**, *24*, 6797−6805.

(5) Haes, A. J.; Zou, S.; Zhao, J.; Schatz, G. C.; Van Duyne, R. P. Localized Surface Plasmon Resonance Spectroscopy near Molecular Resonances. *J. Am. Chem. Soc.* **2006**, *128*, 10905−10914.

(6) Antosiewicz, T. J.; Apell, S. P.; Shegai, T. Plasmon−Exciton Interactions in a Core−Shell Geometry: From Enhanced Absorption to Strong Coupling. *ACS Photonics* **2014**, *1*, 454−463.

(7) Shegai, T.; Miljković, V. D.; Bao, K.; Xu, H.; Nordlander, P.; Johansson, P.; Käll, M. Unidirectional Broadband Light Emission from Supported Plasmonic Nanowires. *Nano Lett.* **2011**, *11*, 706−711.

(8) Nagpal, P.; Lindquist, N. C.; Oh, S.-H.; Norris, D. J. Ultrasmooth Patterned Metals for Plasmonics and Metamaterials. *Science* **2009**, *325*, 594−597.

(9) Novo, C.; Funston, A. M.; Pastoriza-Santos, I.; Liz-Marzán, L. M.; Mulvaney, P. Influence of the Medium Refractive Index on the Optical Properties of Single Gold Triangular Prisms on a Substrate. *J. Phys. Chem. C* **2008**, *112*, 3−7.

(10) Gordon, R.; Brolo, A. G.; Sinton, D.; Kavanagh, K. L. Resonant Optical Transmission through Hole-Arrays in Metal Films: Physics and Applications. *Laser Photonics Rev.* **2010**, *4*, 311−335.

(11) Gordon, R.; Sinton, D.; Kavanagh, K. L.; Brolo, A. G. A New Generation of Sensors Based on Extraordinary Optical Transmission. *Acc. Chem. Res.* **2008**, *41*, 1049−1057.

(12) Brolo, A. G.; Gordon, R.; Leathem, B.; Kavanagh, K. L. Surface Plasmon Sensor Based on the Enhanced Light Transmission through Arrays of Nanoholes in Gold Films. *Langmuir* **2004**, *20*, 4813−4815.

(13) Svedendahl, M.; Chen, S.; Dmitriev, A.; Käll, M. Refractometric Sensing Using Propagating *versus* Localized Surface Plasmons: A Direct Comparison. *Nano Lett.* **2009**, *9*, 4428−4433.

(14) Brolo, A. G.; Arctander, E.; Gordon, R.; Leathem, B.; Kavanagh, K. L. Nanohole-Enhanced Raman Scattering. *Nano Lett.* **2004**, *4*, 2015−2018.

(15) Aouani, H.; Mahboub, O.; Bonod, N.; Devaux, E.; Popov, E.; Rigneault, H.; Ebbesen, T. W.; Wenger, J. Bright Unidirectional Fluorescence Emission of Molecules in a Nanoaperture with Plasmonic Corrugations. *Nano Lett.* **2011**, *11*, 637−644.

(16) Verre, R.; Yang, Z. J.; Shegai, T.; Käll, M. Optical Magnetism and Plasmonic Fano Resonances in Metal−Insulator−Metal Oligomers. *Nano Lett.* **2015**, *15*, 1952−1958.

(17) Francescato, Y.; Giannini, V.; Maier, S. A. Plasmonic Systems Unveiled by Fano Resonances. *ACS Nano* **2012**, *6*, 1830−1838.

(18) Barnes, W. L.; Murray, W. A.; Dintinger, J.; Devaux, E.; Ebbesen, T. W. Surface Plasmon Polaritons and Their Role in the Enhanced Transmission of Light through Periodic Arrays of Subwavelength Holes in a Metal Film. *Phys. Rev. Lett.* **2004**, *92*, 107401.

(19) Przybilla, F.; Degiron, A.; Laluet, J.-Y.; Genet, C.; Ebbesen, T. W. Optical Transmission in Perforated Noble and Transition Metal Films. *J. Opt. A: Pure Appl. Opt.* **2006**, *8*, 458−463.

(20) Martín-Moreno, L.; García-Vidal, F. J.; Lezec, H. J.; Pellerin, K. M.; Thio, T.; Pendry, J. B.; Ebbesen, T. W. Theory of Extraordinary Optical Transmission through Subwavelength Hole Arrays. *Phys. Rev. Lett.* **2001**, *86*, 1114−1117.

(21) López-Tejeira, F.; Rodrigo, S. G.; Martín-Moreno, L.; García-Vidal, F. J.; Devaux, E.; Ebbesen, T. W.; Krenn, J. R.; Radko, I. P.; Bozhevolnyi, S. I.; González, M. U.; Weeber, J. C.; Dereux, A. Efficient Unidirectional Nanoslit Couplers for Surface Plasmons. *Nat. Phys.* **2007**, *3*, 324−328.

(22) Zhou, Y.-S.; Gu, B.-Y.; Wang, H.-Y.; Lan, S. Multi-Reflection Process of Extraordinary Optical Transmission in a Single Subwavelength Metal Slit. *Europhys. Lett.* **2009**, *85*, 24005.

(23) Boller, K.-J.; Imamoğlu, A.; Harris, S. E. Observation of Electromagnetically Induced Transparency. *Phys. Rev. Lett.* **1991**, *66*, 2593−2596.

(24) Zhang, S.; Genov, D. A.; Wang, Y.; Liu, M.; Zhang, X. Plasmon-Induced Transparency in Metamaterials. *Phys. Rev. Lett.* **2008**, *101*, 047401.

(25) Weis, P.; Garcia-Pomar, J. L.; Beigang, R.; Rahm, M. Hybridization Induced Transparency in Composites of Metamaterials and Atomic Media. *Opt. Express* **2011**, *19*, 23573−23580.

(26) Adato, R.; Artar, A.; Erramilli, S.; Altug, H. Engineered Absorption Enhancement and Induced Transparency in Coupled Molecular and Plasmonic Resonator Systems. *Nano Lett.* **2013**, *13*, 2584−2591.

(27) Rodrigo, S. G.; García-Vidal, F. J.; Martín-Moreno, L. Theory of Absorption-Induced Transparency. *Phys. Rev. B: Condens. Matter Mater. Phys.* **2013**, *88*, 155126.

(28) Rodrigo, S. G.; Martín-Moreno, L. Absorption-Induced Transparency Metamaterials in the Terahertz Regime. *Opt. Lett.* **2016**, *41*, 293−296.

(29) Yeh, W.-H.; Petefish, J. W.; Hillier, A. C. Resonance Quenching and Guided Modes Arising from the Coupling of Surface Plasmons with a Molecular Resonance. *Anal. Chem.* **2012**, *84*, 1139−1145.

(30) Ghaemi, H. F.; Thio, T.; Grupp, D. E.; Ebbesen, T. W.; Lezec, H. J. Surface Plasmons Enhance Optical Transmission through Subwavelength Holes. *Phys. Rev. B: Condens. Matter Mater. Phys.* **1998**, *58*, 6779−6782.

(31) Rodrigo, S. G.; García-Vidal, F. J.; Martín-Moreno, L. Influence of Material Properties on Extraordinary Optical Transmission through Hole Arrays. *Phys. Rev. B: Condens. Matter Mater. Phys.* **2008**, *77*, 075401.

DOI: 10.1021/acsnano.6b00709
ACS Nano XXXX, XXX, XXX−XXX

(32) Rodrigo, S. G. *Optical Properties of Nanostructured Metallic Systems*; Springer Theses, Springer-Verlag: Berlin Heidelberg, 2012.
(33) Jackson, J. D. *Classical Electrodynamics*, 2nd ed.; Wiley: New York, 1975.
(34) Przybilla, F.; Genet, C.; Ebbesen, T. W. Long vs. Short-Range Orders in Random Subwavelength Hole Arrays. *Opt. Express* **2012**, *20*, 4697−4709.

DOI: 10.1021/acsnano.6b00709
ACS Nano XXXX, XXX, XXX−XXX